Available online at www.sciencedirect.com
SCIENCE DIRECT®
International Journal of Solids and Structures 43 (2006) 3306–3323
INTERNATIONAL JOURNAL OF SOLIDS and STRUCTURES
www.elsevier.com/locate/ijsolstr

Continuum-mechanical modelling of kink-band formation in fibre-reinforced composites

Y.B. Fu [a,*], Y.T. Zhang [b]

[a] Department of Mathematics, Keele University, Staffordshire ST5 5BG, UK
[b] Department of Mechanics, Tianjin University, Tianjin 300072, China

Received 17 February 2005; received in revised form 18 May 2005
Available online 15 July 2005

Abstract

A kink is a singular surface across which the displacement is continuous but the deformation gradient and the fibre direction suffer a discontinuity. A kink band is a highly deformed or even damaged region bounded by two kinks. The objective of modelling kink-band formation, within the framework of finite elasticity theory, is to find a suitable strain–energy function, guided by results from a finite number of simple experiments, that can be used to predict what have been observed and what might be possible under other loading conditions. In this paper, we explain a theoretical basis for choosing such strain–energy functions. More precisely, for a given strain–energy function that allows formation of kinks and a given deformation field, we characterize all possible deformation fields that can join the given deformation field through a kink and explain a procedure that can be used to assess the stability properties of any kink solution that is mathematically possible. In contrast with most previous studies in the engineering community where, for instance, the kink orientation angle is undetermined, the present theory completely determines the kink propagation stress, the kink orientation angle and the fibre direction within the kink band.

Keywords: Kink bands; Fibre-reinforced composites; Strong ellipticity; Stability; Nonlinear elasticity

1. Introduction

It is now widely recognized that kink-band formation and propagation is the dominant compression failure mechanism in unidirectionally fibre-reinforced composites. Typically, when such a composite with an initial imperfection is compressed, the load curve consists of an initiation (peak) stress followed by a much

* Corresponding author. Tel.: +44 1782 583650; fax: +44 1782 584268.
E-mail addresses: y.fu@keele.ac.uk (Y.B. Fu), ytzhang@tju.edu.cn (Y.T. Zhang).

0020-7683/$ - see front matter
doi:10.1016/j.ijsolstr.2005.05.031

lower steady propagation stress; see, for instance, Sutcliffe and Fleck (1994), Kyriakides et al. (1995), Moran et al. (1995), Sivashanker et al. (1996), Liu et al. (1996), Moran and Shih (1998), and Vogler and Kyriakides (1999, 2001). The initiation stress is known to be quite sensitive to imperfections such as initial waviness or misalignment of fibres and fibre breakage due to micro-buckling, but the constant propagation stress, at which the kinked fibres ''lock-up'' into a fixed orientation and the kink band may propagate steadily, seems to be a material property independent of such imperfections. For various engineering theories that are aimed at predicting the initiation stress, the propagation stress, the kink orientation angle and the fibre direction within the kink band, we refer the reader to Yin (1992), Grandidier et al. (1992), Guynn et al. (1992), Budiansky and Fleck (1993, 1994), Chung and Weitsman (1995), Schapery (1995), Dao and Asaro (1996), Fleck (1997), Jensen and Christoffersen (1997), Kyriakides and Ruff (1997), Vogler and Kyriakides (1997), Budiansky et al. (1998), Berbinau et al. (1999), Hsu et al. (1999), Jensen (1999), Drapier et al. (2001), Vogler et al. (2001), and the references therein. We also mention the papers by Hunt et al. (2000) and Wadee et al. (2004) that are concerned with kink-band instability in layered structures in which sliding is permitted between the layers. Because kink banding in the latter layered structures can be initiated much more easily, the experimental and analytical results given by the last two papers do not suffer the diversity and uncertainty associated with those results on traditional fibre-reinforced composites. We believe that their results are indicative of what might be expected in traditional fibre-reinforced composites in an idealized situation (that is without any imperfections): kink-band formation, unlike Eulerian buckling, is not an incremental process; rather, it is dynamic and the kinked configuration is an energetically preferred configuration that cannot be reached from the initial configuration by a quasi-static loading process. This point of view is consistent with the established view in the engineering community that kink-band formation is initiated, through imperfections, by a limit-load instability, and the load against end-shortening curve typically has the unique *snap-back* behaviour (compare Fleck's, 1997, Fig. 12(b) with Hunt et al.'s, 2000, Fig. 3).

A unidirectionally fibre-reinforced composite can be modelled as a transversely isotropic elastic material. Although a rational continuum mechanics theory for such composites has been in existence for more than three decades, see Spencer (1972), and despite its success in solving a large number of boundary-value problems, it is only recently that a first attempt has been made in using this theory to explain kink-band formation; see Merodio and Pence (2001a,b), Merodio and Ogden (2002, 2003a,b, 2005).

Following Merodio and Pence (2001a,b), we also view kink-band formation as a phase transformation problem. Although plastic deformation usually occurs inside a kink band, as long as unloading does not take place, we may view the materials inside and outside the kink band as two phases of the same elastic material.

Once kink-band formation is viewed as an elastic phase-transformation problem, we may then draw upon the vast expertise that has accrued during recent decades on the modelling of stress induced phase transformations. The most attractive feature of this approach is that we only need to find an appropriate strain–energy function. Once such a strain–energy function is found, no ad hoc approximations need to be made and all the required results, such as the kink propagation stress, the kink orientation angle and the fibre direction within the kink band, follow as mathematical consequences.

It is now known that a necessary condition for a stress-induced phase transformation (and hence kink-band formation) to be possible is that the strain–energy function, as a function of the deformation gradient, losses strong ellipticity at some deformation gradients; see Knowles and Sternberg (1978). Strong ellipticity of transversely isotropic materials has been the focus of some recent studies; see Qiu and Pence (1997), Merodio and Pence (2001a,b), Merodio and Ogden (2002, 2003a,b, 2005), and Walton and Wilber (2003).

A major difference between the present study and the studies of Merodio and Pence (2001a,b) is that in our present study the Maxwell relation (i.e., zero kink-driving traction) is used as an equilibrium condition, whereas in Merodio and Pence (2001a,b) satisfaction of the Maxwell relation is viewed as corresponding to neutral stability and this relation does not play as an important role as in our study. In fact, it is through the use of this relation that we are able to determine completely the kink propagation stress, the kink orientation angle and the fibre direction within the kink band. In this respect, our approach follows that of Freidin and Chiskis (1994a,b), Freidin et al. (2002) and Fu and Freidin (2004) in their studies of stress-induced phase transformations, and bears the same spirit as that of Hunt et al. (2000) who use the Maxwell relation as a stability criterion. In this connection, we also mention a recent study by Jensen (1999) where a work-balance relation $W^{\mathrm{I}} = W^{\mathrm{E}}$ is used in the determination of the orientation angle of kinked fibres at lock-up, where W^{I} is the work done per unit volume by the stresses in the kink band and W^{E} is the work done per unit volume by the external loads as the kink band broadens. Since the Maxwell relation can be interpreted as a necessary condition for the total energy to be stationary with respect to perturbations of the kink position in the undeformed configuration (see, for instance, Abeyaratne, 1983), a possible connection between the Maxwell relation and Jensen's (1999) work-balance relation may exist and remains to be established.

We observe that in the recent studies by Merodio and Ogden (2002, 2003a,b, 2005), marginal violation of the strong ellipticity condition is viewed as corresponding to fibre kinking. This point of view has also previously been adopted by some researchers in the engineering community; see, e.g., Christoffersen and Jensen (1996). Clearly, these studies are concerned with the prediction of the initiation/peak stress corresponding to the onset of failure, and the normal to the kink predicted by such theories is simply the normal to a characteristic surface (a weak discontinuity surface) which may not be the normal to a fully developed, steadily propagating kink which is a strong discontinuity (shock) surface. In the present study, our concern is not with the initiation stress. Instead, our main concern is with the prediction of the kink propagation stress, the kink orientation angle and the fibre direction in a fully developed kink band. Such a fully developed kink band corresponds to a fully nonlinear solution of the governing equations and may develop, under large amplitude perturbations, well before the strong ellipticity condition is violated even in the absence of imperfections.

The rest of this paper is organized into four sections as follows. After stating the governing equations in Section 2, we show in Section 3, using a simple model energy function, how the kink orientation angle and the deformation field in the kink band can be determined completely with the use of the jump conditions that must be satisfied across an equilibrium kink. A good theoretical model should also be able to predict what is observed in experiments. Thus, if a fully developed kink band is observed to be stable with respect to small-amplitude perturbations, our model should at least predict stability with respect to Weierstrass-type perturbations and interfacial perturbations. Stability with respect to the former requires satisfaction of the ellipticity (or Legendre–Hadamard) condition by the deformation gradient throughout the elastic body. We satisfy this requirement by imposing the slightly stronger assumption of strong ellipticity. Stability with respect to interfacial perturbations is discussed in Section 4 where we derive a simple formula as a test criterion and carry out some illustrative calculations. The paper is concluded with a summary and some additional comments.

2. Governing equations

In this paper, we are concerned with a macroscopic description of unidirectionally fibre-reinforced composites, that is, we take the fibres and matrix material as a whole continuum and we assume that its continuum mechanical behaviour is known. We view a kink in a fibre-reinforced composite as a strong discontinuity surface, or equivalently a static shock, across which the displacement field is continuous but the deformation gradient suffers a discontinuity. Let the static deformation of a fibre-reinforced composite be given by

$$\mathbf{x} = \mathbf{x}(\mathbf{X}), \tag{2.1}$$

which assigns position $\mathbf{x}$ to the material point that occupies position $\mathbf{X}$ in the undeformed (reference) configuration. We assume that $\mathbf{x}$ and $\mathbf{X}$ have coordinates x_i and X_A, respectively, relative to a common rectangular coordinate system. We shall follow the convention that lower case subscripts are associated with the coordinates of $\mathbf{x}$ and upper case subscripts with the coordinates of $\mathbf{X}$. The jump of a function f across a kink is defined by

$$[f] = f^+ - f^-, \tag{2.2}$$

where superscripts "+" and "−" signify evaluation at the kink as it is approached from the two sides respectively. To avoid using double superscripts, we shall replace a superscript "+" or "−" by the corresponding subscript on quantities that have already another superscript. Thus, for instance, f^+ and g_+^2 both signify evaluation on the "+" side of a kink. When there is no "+" or "−" superscript/subscript attached to a field variable evaluated at the kink, it means that the variable can be evaluated on either side of the kink. In most of our analysis, the "+" and "−" sides take the same footing, but to fix ideas, we may take the "+" side to correspond to the kink-band side; see Fig. 1.

The behaviour of an incompressible elastic body is completely described by its strain–energy function W which is taken to be a C^2 function of the deformation gradient $\mathbf{F}$. Thus, we write $W = W(\mathbf{F})$, where

$$\mathbf{F} = \frac{\partial \mathbf{x}}{\partial \mathbf{X}}, \qquad F_{iA} = x_{i,A}, \tag{2.3}$$

and a comma signifies partial differentiation. The first Piola–Kirchhoff stress tensor $\boldsymbol{\pi}$ is given by

$$\boldsymbol{\pi}^{\mathrm{T}} = \frac{\partial W}{\partial \mathbf{F}} - p\mathbf{F}^{-1}, \qquad \pi_{iA} = \frac{\partial W}{\partial F_{iA}} - pF_{Ai}^{-1}, \tag{2.4}$$

where p is the pressure associated with the constraint of incompressibility. The equilibrium equation is given by

$$\mathrm{Div}\,\boldsymbol{\pi}^{\mathrm{T}} = \mathbf{0}, \qquad \pi_{iA,A} = 0, \tag{2.5}$$

and its weak form is

$$[\boldsymbol{\pi}\mathbf{N}] = \mathbf{0}, \qquad [\pi_{iA}N_A] = 0, \tag{2.6}$$

where $\mathbf{N}$ denotes the unit vector normal to the kink in the reference configuration and points from the "+" phase into the "−" phase. The jump condition (2.6) expresses continuity of traction across the kink.

It is well-known that continuity of displacement implies that the jump $[\mathbf{F}]$ may be written as

$$[\mathbf{F}] = \mathbf{f} \otimes \mathbf{N}, \tag{2.7}$$

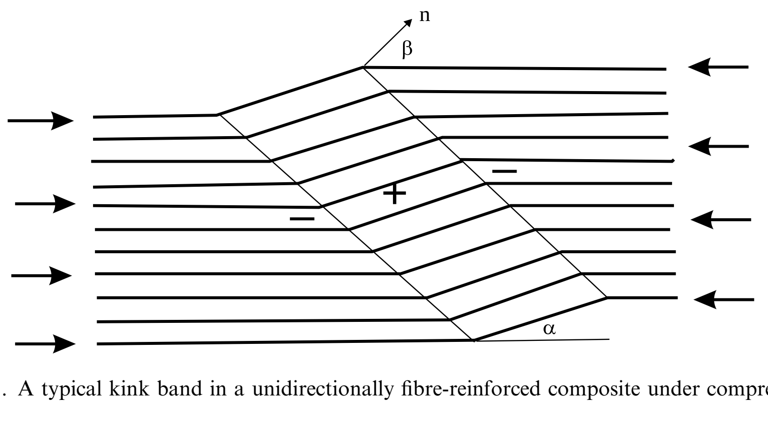

Fig. 1. A typical kink band in a unidirectionally fibre-reinforced composite under compression.

where $\mathbf{f}$, defined by

$$\mathbf{f} = [\mathbf{F}]\mathbf{N}, \tag{2.8}$$

may be referred to as the amplitude of the jump in [**F**]. We also impose the additional condition

$$[W] - \mathbf{f} \cdot \boldsymbol{\pi}\mathbf{N} = 0, \tag{2.9}$$

which will be shown in Section 4 to be necessary for the energy functional to be stationary with respect to perturbations of the kink position in the reference configuration (see, e.g., Abeyaratne, 1983). Any static deformation containing a kink must satisfy the equilibrium equation (2.5) away from the kink and must satisfy the jump conditions (2.6), (2.7) and (2.9) across the kink.

It is found to be more convenient to express the jump conditions (2.6), (2.7) and (2.9) in terms of the Cauchy stress tensor $\boldsymbol{\sigma} = \mathbf{F}\boldsymbol{\pi}^{\mathrm{T}}$ and the unit normal $\mathbf{n}$ to the kink in the deformed configuration. We then have

$$[\mathbf{F}] = (\mathbf{c} \otimes \mathbf{n})\mathbf{F}^{-} = (\mathbf{c} \otimes \mathbf{n})\mathbf{F}^{+}, \tag{2.10}$$

$$[\boldsymbol{\sigma}]\mathbf{n} = \mathbf{0}, \tag{2.11}$$

$$[W] - \mathbf{c} \cdot \boldsymbol{\sigma}\mathbf{n} = 0, \tag{2.12}$$

where

$$\mathbf{c} = \frac{1}{|\mathbf{F}^{\mathrm{T}}\mathbf{n}|}\mathbf{f}. \tag{2.13}$$

We note that $\mathbf{F}^{\mathrm{T}}\mathbf{n}$, and hence $\mathbf{c}$, are continuous across the kink. This follows from Nanson's formula $\mathbf{F}^{\mathrm{T}}\mathbf{n}\,\mathrm{d}a = \mathbf{N}\,\mathrm{d}A$, where $\mathrm{d}A$ and $\mathrm{d}a$ are two corresponding area elements in the undeformed and deformed configurations, respectively. The counterparts of (2.10)–(2.13) for compressible materials were the basic relations employed by Freidin et al. (2002) in studying stress-induced phase transformations (see also Fu and Freidin, 2004).

The elastic moduli $\mathscr{A}^{+}_{jilk}$ and $\mathscr{A}^{-}_{jilk}$ are defined by

$$\mathscr{A}^{+}_{jilk} = F^{+}_{jA}F^{+}_{lB}\left.\frac{\partial^2 W}{\partial F_{iA}\,\partial F_{kB}}\right|_{\mathbf{F}=\mathbf{F}^{+}}, \qquad \mathscr{A}^{-}_{jilk} = F^{-}_{jA}F^{-}_{lB}\left.\frac{\partial^2 W}{\partial F_{iA}\,\partial F_{kB}}\right|_{\mathbf{F}=\mathbf{F}^{-}}. \tag{2.14}$$

The experimental results of Kyriakides et al. (1995), Moran et al. (1995) and Moran and Shih (1998) show that when a kink band is fully developed, the kinks may propagate at a constant stress known as the propagation stress. Using the terminology of theory of phase transformations, we may also refer to the propagation stress as the Maxwell stress. We view a fully developed kink band as being neutrally stable (Ericksen, 1975) in the sense that as the kink-band broadens, the total energy of the elastic body remains the same but is less than the energy of any other perturbed configuration. Thus, the kink band which we try to model should be stable at least with respect to Weierstrass-type perturbations (see Cherkaev, 1991, p. 151) and interfacial perturbations. Stability with respect to Weierstrass-type perturbations is guaranteed by strong ellipticity in both "+" and "−" phases:

$$\mathscr{A}^{\pm}_{jilk}c_j d_i c_l d_k > 0 \quad \text{for all nonzero vectors } \mathbf{c} \text{ and } \mathbf{d} \text{ satisfying } \mathbf{c} \cdot \mathbf{d} = 0. \tag{2.15}$$

Stability with respect to interfacial perturbations will be discussed in Section 4. It is analogous to satisfaction of the complementing condition at a free surface or at the interface between two welded dissimilar elastic bodies (see Simpson and Spector, 1989, 1991; Mielke and Sprenger, 1998).

3. A model strain–energy function and kinked solutions

It is well-known (see, e.g., Spencer, 1972) that the strain–energy function W for a generally incompressible, transversely isotropic material depends on the four invariants defined by

$$I_1 = \mathrm{tr}\,\mathbf{C}, \quad I_2 = \mathrm{tr}\,\mathbf{C}^{-1}, \quad I_4 = \mathbf{A}\cdot(\mathbf{CA}) = \mathbf{a}\cdot\mathbf{a}, \quad I_5 = \mathbf{A}\cdot(\mathbf{C}^2\mathbf{A}) = \mathbf{a}\cdot\mathbf{Ba},$$

where $\mathbf{C} = \mathbf{F}^{\mathrm{T}}\mathbf{F}$, $\mathbf{B} = \mathbf{FF}^{\mathrm{T}}$, $\mathbf{a} = \mathbf{FA}$, and $\mathbf{A}$ is the unit vector along the fibre direction in the undeformed configuration. From $\boldsymbol{\sigma} = \mathbf{F}\partial W/\partial\mathbf{F} - p\mathbf{I}$, we obtain

$$\boldsymbol{\sigma} = 2(W_1 + W_2 I_1)\mathbf{B} - 2W_2\mathbf{B}^2 + 2W_4(\mathbf{a}\otimes\mathbf{a}) + 2W_5(\mathbf{a}\otimes\mathbf{Ba} + \mathbf{Ba}\otimes\mathbf{a}) - p\mathbf{I}, \tag{3.1}$$

where $W_1 = \partial W/\partial I_1, W_4 = \partial W/\partial I_4$, etc. In this study we consider a class of incompressible fibre-reinforced composites that is modelled by the strain–energy function

$$W = \frac{1}{2}(I_1 - 1) + \frac{1}{2}\gamma_1(I_4 - 1)^2 + \frac{1}{3}\gamma_2(I_4 - 1)^3, \tag{3.2}$$

where γ_1 and γ_2 are material constants and we have scaled the energy function such that the first term does not contain a material constant. The second term involving γ_1 above has previously been used by Triantafyllidis and Abeyaratne (1983), Qiu and Pence (1997), Merodio and Ogden (2002, 2003a) to account for the existence of a unidirectional reinforcing in an otherwise isotropic matrix material. We observe that the term involving γ_2 in (3.2) breaks the symmetry in the strain–energy function with respect to extension ($I_4 - 1 > 0$) and compression ($I_4 - 1 < 0$) along the fibre direction. We use this term to reflect the fact that in the large deformation regime, a typical unidirectionally fibre-reinforced composite does respond differently under compression from when it is under tension along the fibre direction.

Corresponding to (3.2), Eq. (3.1) reduces to

$$\boldsymbol{\sigma} = \mathbf{B} + 2\{\gamma_1(I_4 - 1) + \gamma_2(I_4 - 1)^2\}(\mathbf{a}\otimes\mathbf{a}) - p\mathbf{I}. \tag{3.3}$$

We shall focus on the simplest case when the deformation is plane-strain, the X_1-axis is along the undeformed fibre direction, and $\mathbf{F}^-$ takes the simple form

$$\mathbf{F}^- = \begin{pmatrix} \lambda & 0 \\ 0 & \lambda^{-1} \end{pmatrix}, \tag{3.4}$$

where λ is a constant. This deformation may be viewed as the deformation before any kink band has formed. Our first task is to determine at what values of λ, as it is varied away from unity, formation of kinks first becomes possible.

To the above end, we first assume that a kink with normal $\mathbf{n} = (n_1, n_2)^{\mathrm{T}}$ has already formed. This kink joins $\mathbf{F}^-$ given by (3.4) and $\mathbf{F}^+$ that is to be determined. From (2.10) and the incompressibility condition $\det\mathbf{F}^{\pm} = 1$ it may be deduced that $\mathbf{c}\cdot\mathbf{n} = 0$. Thus, we may write

$$\mathbf{c} = k\mathbf{m}, \quad \text{where } \mathbf{m} = (n_2, -n_1)^{\mathrm{T}} \tag{3.5}$$

and k is to be determined. We note that the trivial solution $k = 0$ is always a solution, but we are looking for a *fully nonlinear* nontrivial solution (that is, k is not necessarily small).

In terms of k, the unknown $\mathbf{F}^+$ can be calculated with the aid of (2.10) and $[\boldsymbol{\sigma}]$ can be evaluated with the aid of (3.3). The jump conditions (2.11) and (2.12) give us three scalar equations that can be used to determine the three unknowns k, n_1 and p^+. For an arbitrary choice of the strain–energy function, it is quite possible that these three equations do not have any real solutions at all. It is now known from the theory of phase transformations that a necessary condition for such a real solution to exist is that the strain–energy function loses strong ellipticity for some deformation gradients. Even when this condition is satisfied, a real solution can be found only for some *admissible* values of λ. Our first task is to characterize such admissible deformations.

By eliminating $[p]$ from the two scalar equations obtained from (2.11), we obtain $[\sigma_{1i}]n_in_2 - [\sigma_{2i}]n_in_1 = 0$. To facilitate subsequent analysis, we define a function L through

$$\lambda^{-2}L(k,\mathbf{n},\mathbf{m}) \equiv \frac{1}{k}\{[\sigma_{1i}]n_in_2 - [\sigma_{2i}]n_in_1\} = \frac{1}{k}\{[\sigma_{1i}]n_im_1 + [\sigma_{2i}]n_im_2\}. \tag{3.6}$$

With the use of (2.10), (3.3) and (3.5), we find

$$\begin{aligned} L(k,\mathbf{n},\mathbf{m}) = {} & 1 - 4\lambda^6n_1^4\gamma_1 + 8\lambda^6n_1^4\gamma_2 - 8\lambda^8n_1^4\gamma_2 \\ & + n_1^2\big((-2\lambda^4 + 6\lambda^6)\gamma_1 + (-1+\lambda^2)(1+\lambda^2+2\lambda^4(-1+5\lambda^2)\gamma_2)\big) \\ & + k\big(-8\lambda^8n_1^5n_2\gamma_2 + 2\lambda^6n_1^3n_2(3\gamma_1 + 2(-3+5\lambda^2)\gamma_2)\big) \\ & + k^2\big(2\lambda^6n_1^4\gamma_1 + 4\lambda^6(-1+5\lambda^2)n_1^4\gamma_2 - 16\lambda^8n_1^6\gamma_2\big) + 10k^3\lambda^8n_1^5n_2\gamma_2 + 2k^4\lambda^8n_1^6\gamma_2 = 0. \end{aligned} \tag{3.7}$$

This is a quadratic equation in terms of k. It can be shown with the aid of Mathematica that the jump condition (2.12), after division by k^2, yields another quartic equation for k:

$$\begin{aligned} & 3 - 12\lambda^6n_1^4\gamma_1 + 24\lambda^6n_1^4\gamma_2 - 24\lambda^8n_1^4\gamma_2 + 3n_1^2((-2\lambda^4+6\lambda^6)\gamma_1 + (-1+\lambda^2)(1+\lambda^2+2\lambda^4(-1+5\lambda^2)\gamma_2)) \\ & \quad + k(-16\lambda^8n_1^5n_2\gamma_2 + 4\lambda^6n_1^3n_2(3\gamma_1 + 2(-3+5\lambda^2)\gamma_2)) \\ & \quad + k^2(3\lambda^6n_1^4\gamma_1 + 6\lambda^6(-1+5\lambda^2)n_1^4\gamma_2 - 24\lambda^8n_1^6\gamma_2) + 12\lambda^8n_1^5n_2\gamma_2k^3 + 2\lambda^8n_1^6\gamma_2k^4 = 0. \end{aligned} \tag{3.8}$$

With the aid of the command *Resultant* in Mathematica, it can be shown that these two polynomial equations for k will have a common root only if

$$L(0,\mathbf{n},\mathbf{m})f(\lambda^2,n_1^2)g(\lambda^2,n_1^2) = 0, \tag{3.9}$$

where the functions f and g are defined by

$$\begin{aligned} f(x,y) = {} & 1 - y + x^4y - 2x^4y\gamma_1 + 2x^6y\gamma_1 + 2x^4y\gamma_2 - 4x^6y\gamma_2 + 2x^8y\gamma_2, \\ g(x,y) = {} & 64\gamma_2^2 - 72(-1+x)x^4y^4\gamma_2^3(1+x+2x^2\gamma_1 + 2(-1+x)x^2\gamma_2) \\ & - 6x^3y^3\gamma_2(-(x^2\gamma_1^3) + 42(-1+x)x^2\gamma_1^2\gamma_2 \\ & + 4\gamma_2^2(3(4-x-4x^2+2x^3) + 2(-1+x)^2x^2(-11+5x)\gamma_2) \\ & + 12(-1+x)\gamma_1\gamma_2(2(1+x) + x^2(-11+7x)\gamma_2)) \\ & + 8y\gamma_2(-6x^2\gamma_1^2 + 2x^2(-4+13x)\gamma_1\gamma_2 + \gamma_2(16(-1+x^2) + x^2(8-52x+35x^2)\gamma_2)) \\ & + y^2(9x^4\gamma_1^4 - 6x^4(-4+5x)\gamma_1^3\gamma_2 + 4(-1+x)x^2\gamma_1^2\gamma_2(-12(1+x) + x^2(2+61x)\gamma_2) \\ & + 8x^2\gamma_1\gamma_2^2(8 - 44x - 8x^2 + 26x^3 + x^2(-4+111x-192x^2+85x^3)\gamma_2) \\ & + 8\gamma_2^2(8(-1+x^2)^2 + x^2(-8+88x-45x^2-52x^3+35x^4)\gamma_2 \\ & + 2(-1+x)^2x^4(1-35x+25x^2)\gamma_2^2)). \end{aligned}$$

We note from (2.10) and (3.6) that

$$\lambda^{-2}L(0,\mathbf{n},\mathbf{m}) = \lim_{k\to 0}\frac{1}{k}[\sigma_{ji}]n_im_j = \lim_{k\to 0}\frac{\mathrm{d}}{\mathrm{d}k}\sigma_{ij}^{+}n_im_j = \mathscr{A}_{jilk}^{-}n_jn_lm_im_k, \tag{3.10}$$

where use has also been made of (2.14) and (3.5). It is then seen that the strong ellipticity condition (2.15) applied to the "−" phase is given by

$$L(0,\mathbf{n},\mathbf{m}) = 1 - 4\lambda^6 n_1^4(\gamma_1 + 2(-1+\lambda^2)\gamma_2) + n_1^2((-2\lambda^4 + 6\lambda^6)\gamma_1 + (-1+\lambda^2)(1+\lambda^2+2\lambda^4(-1+5\lambda^2)\gamma_2)) > 0. \tag{3.11}$$

The boundary of strong ellipticity is given by $L(0,\mathbf{n},\mathbf{m}) = 0$. The strong ellipticity for the "+" phase (i.e., the kink band) is dependent on k; we shall discuss how it can be verified numerically later.

At this juncture, it is appropriate to discuss the choice of the material constants γ_1 and γ_2. First, it follows from (3.3) that for uniaxial extension in the fibre direction (which is chosen to be in the x_1-direction) we have

$$\pi_{11} = \lambda + 2\gamma_1\lambda(\lambda^2-1) + 2\gamma_2\lambda(\lambda^2-1)^2 - \lambda^{-3},$$

which, for small $|\lambda - 1|$, yields

$$\pi_{11} = 4(\gamma_1+1)(\lambda-1) + \mathrm{O}((\lambda-1)^2).$$

Thus, for a physically realistic response, we impose the condition

$$\gamma_1 > -1. \tag{3.12}$$

Next, guided by existing experimental evidence, we require our model to predict that fibre-kinking will not take place in uniaxial extension. Thus, we require strong ellipticity to be satisfied for all $\lambda \geqslant 1$. We view $L(0,\mathbf{n},\mathbf{m})$ as a quadratic function of n_1^2 defined in the interval $n_1^2 \in [0,1]$. This function equals 1 at $n_1^2 = 0$ and

$$\lambda^4\{1 + 2\gamma_1(\lambda^2-1) + 2\gamma_2(\lambda^2-1)^2\} \tag{3.13}$$

at $n_1^2 = 1$. It is easy to show that the expression in (3.13) is positive for all $\lambda \geqslant 1$ if and only if

$$\gamma_2 \geqslant 0, \qquad \gamma_1 > -\sqrt{2\gamma_2}. \tag{3.14}$$

There is the possibility that L has a local minimum in the interval $0 < n_1^2 < 1$, but this will occur only if the following three conditions are simultaneously satisfied:

$$-\gamma_1 - 2(\lambda^2-1)\gamma_2 > 0, \tag{3.15}$$

$$(-2\lambda^4 + 6\lambda^6)\gamma_1 + (-1+\lambda^2)(1+\lambda^2+2\lambda^4(-1+5\lambda^2)\gamma_2) < 0, \tag{3.16}$$

$$-2\lambda^4(1+\lambda^2)\gamma_1 - (-1+\lambda^2)(-1-\lambda^2+2\lambda^4(1+3\lambda^2)\gamma_2) > 0. \tag{3.17}$$

The expressions in the three conditions above correspond to the coefficient of n_1^4 in L and the derivatives of L with respect to n_1^2 at $n_1^2 = 0, 1$. When these conditions hold, we require the local minimum to be positive for $\lambda \geqslant 1$, that is

$$1 + \frac{(2\lambda^4(-1+3\lambda^2)\gamma_1 + (-1+\lambda^2)(1+\lambda^2+2\lambda^4(-1+5\lambda^2)\gamma_2))^2}{16\lambda^6(\gamma_1 + 2(-1+\lambda^2)\gamma_2)} > 0. \tag{3.18}$$

It does not seem possible to find the precise necessary conditions on γ_1, γ_2 that ensure the satisfaction of (3.18) for $\lambda \geqslant 1$. But it is clear from (3.18) that a sufficient condition is $\gamma_1 \geqslant 0$. Summarizing all the above considerations, we impose the conditions

$$\gamma_1 \geqslant 0, \qquad \gamma_2 \geqslant 0, \tag{3.19}$$

which ensure that the strong ellipticity condition cannot be violated for all $\lambda \geqslant 1$.

We now proceed to discuss the solutions of (3.9). The equation $L(0,\mathbf{n},\mathbf{m}) = 0$ from the first factor in (3.9) corresponds to the trivial solution $k = 0$ and should be neglected in our construction of stable kinked solutions. Solving the equation $f(\lambda^2, n_1^2) = 0$ from the second factor, we obtain

$$\gamma_2 = \frac{-1 + n_1^2 - \lambda^4 n_1^2 - 2\lambda^4(-1+\lambda^2)n_1^2\gamma_1}{2\lambda^4(-1+\lambda^2)^2 n_1^2},$$

which is always negative for $0 \leqslant n_1^2 \leqslant 1$, violating our assumption $(3.19)_2$. Thus, the second factor is conveniently dismissed under the assumptions (3.19) and Eq. (3.9) reduces to

$$g(\lambda^2, n_1^2) = 0. \tag{3.20}$$

In Fig. 2, we have shown the solution of (3.20) together with the boundary of strong ellipticity obtained from $L(0, \mathbf{n}, \mathbf{m}) = 0$ for $\gamma_2 = 4.5$ and $\gamma_1 = 0$, 0.01, 0.02, 0.0251. We find that for $\gamma_2 = 4.5$, the closed curve representing the solution of (3.20) shrinks as γ_1 is increased gradually until it completely disappears at about $\gamma_1 = 0.039$. A similar pattern is observed when $\gamma_2 = 5$ in which case a solution only exists up to $\gamma_1 = 0.38$ approximately. Also, we find that for each fixed γ_2, as γ_1 is increased, strong ellipticity begins to be violated by the deformation in the kink band before the solution to (3.20) described above ceases to exist. For instance, for $\gamma_2 = 4.5$, this upper limiting value of γ_1 is approximately 0.02512.

Take $\gamma_1 = 0$ as an example. Fig. 2 shows that as λ is decreased from unity, a kink can form when λ^2 reaches 0.8065. Corresponding to this stretch value we have $n_1^2 = 0.4817$. The corresponding value of k is the common root of (3.7) and (3.8). It can be deduced from (3.7) and (3.8) that if (n_1, n_2, k) is a solution, then so are $(-n_1, n_2, -k)$, $(-n_1, -n_2, k)$ and $(n_1, -n_2, -k)$, but the latter three solutions can be obtained from the first solution by rigid-body rotations. Thus, without loss of generality, we shall focus on the solution with $n_1 \geqslant 0$, $n_2 \geqslant 0$ which correspond to the case shown in Fig. 1. For $\gamma_1 = 0$, we obtain

$$n_1 = 0.6940, \qquad n_2 = 0.7199, \qquad k = -0.1337. \tag{3.21}$$

The kink orientation angle is given by $\beta = \tan^{-1}(n_2/n_1)$ and the fibre direction inside the kink band is characterized by the angle $\alpha = \tan^{-1}(F_{21}^+/F_{11}^+)$. We have

$$\beta \approx 46.0^\circ, \qquad \alpha \approx 3.9^\circ. \tag{3.22}$$

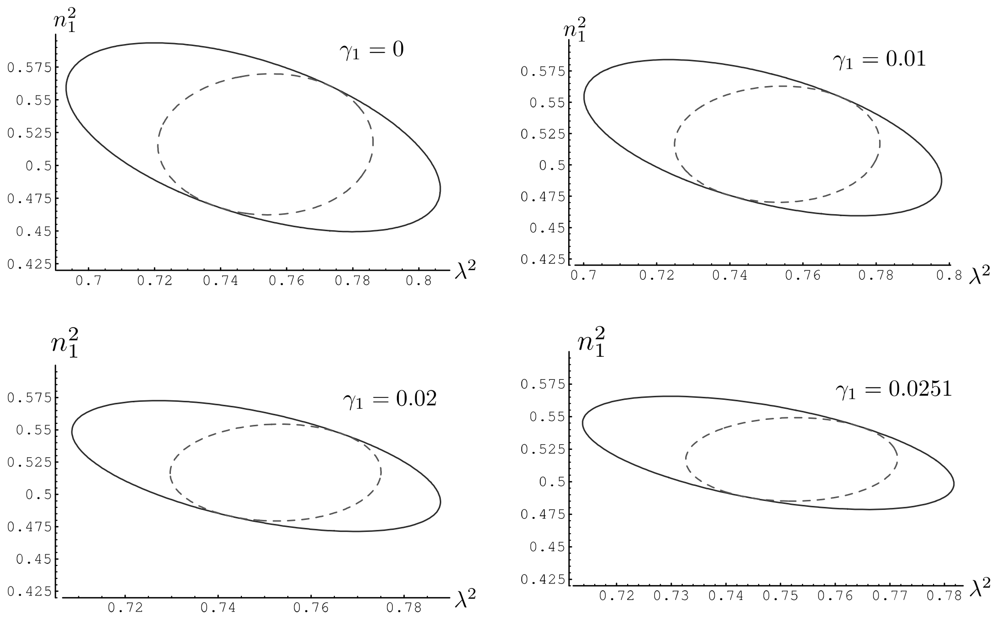

Fig. 2. The solution of (3.20) (solid line) and the boundary of strong ellipticity given by $L(0, \mathbf{n}, \mathbf{m}) = 0$ (dashed line, inside which the strong ellipticity condition is violated) when $\gamma_2 = 4.5$ and γ_1 takes the four different values shown in the plots.

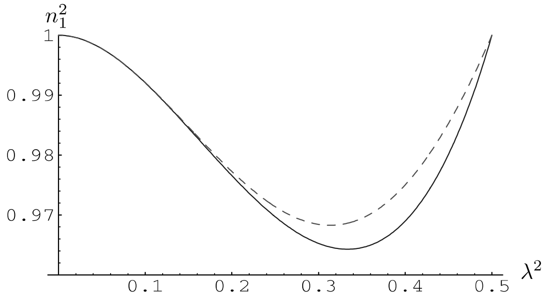

Fig. 3. The solution of (3.24) (solid line) and the boundary of strong ellipticity (dashed line, above which the strong ellipticity condition is violated) when $\gamma_1 = 1$, $\gamma_2 = 0$.

For the other three values of γ_1 shown in Fig. 2, we obtain

$$\begin{aligned} &\gamma_1 = 0.01: \quad n_1 = 0.6982, \quad n_2 = 0.7159, \quad k = -0.1127; \quad \beta = 45.7^\circ, \quad \alpha = 3.3^\circ, \\ &\gamma_1 = 0.02: \quad n_1 = 0.7031, \quad n_2 = 0.7111, \quad k = -0.08778, \quad \beta = 45.3^\circ, \quad \alpha = 2.6^\circ, \\ &\gamma_1 = 0.0251: \quad n_1 = 0.7060, \quad n_2 = 0.7082, \quad k = -0.07257, \quad \beta = 45.1^\circ, \quad \alpha = 2.1^\circ. \end{aligned} \tag{3.23}$$

We observe that for the case $\gamma_1 \neq 0$, $\gamma_2 = 0$, which has previously been studied by Merodio and Pence (2001a,b), Eqs. (3.7) and (3.20) would yield

$$n_1^2 = \frac{1}{1 - (1 - 2\gamma_1)\lambda^4 - 2\gamma_1\lambda^6}, \qquad 2n_2 + kn_1 = 0, \tag{3.24}$$

and the strong ellipticity condition would be represented by

$$L(0, \mathbf{n}, \mathbf{m}) = 1 + (-1 + (1 - 2\gamma_1)\lambda^4 + 6\gamma_1\lambda^6)n_1^2 - 4\gamma_1\lambda^6 n_1^4 > 0. \tag{3.25}$$

It follows from (3.24) that kink-band formation is possible only if $\gamma_1 > 1/2$ and for

$$\lambda^2 \leqslant 1 - \frac{1}{2\gamma_1}. \tag{3.26}$$

When the equality in (3.26) holds, we have $n_1^2 = 1$ and $L(0, \mathbf{n}, \mathbf{m}) = 0$, $k = 0$, see Fig. 3. Thus, as λ is decreased from unity, a kinked solution becomes possible when λ^2 reaches $1 - 1/(2\gamma_1)$, but the kinked solution has zero amplitude and violates the strong ellipticity condition. This implies that this model does not predict a fully developed stable kink.

4. Interfacial stability test

The *primary* kinked deformation determined in the previous section is a stationary point of the energy functional with respect to perturbations of (i) the displacement field, (ii) the kink position in the current configuration, and (iii) the kink position in the reference configuration (as ensured, respectively, by the satisfaction of the equilibrium equation (2.5) and the jump conditions (2.6) and (2.9)). However, it is not yet known whether such a two-phase deformation is an energy minimizer. If it is observed experimentally that the kink band which we are trying to model is stable at least with respect to small-amplitude perturbations, we must make sure that the associated deformation is a local energy minimizer. It is generally difficult to give precise necessary and sufficient conditions for a two-phase deformation to be a local energy minimizer with respect to all possible perturbations/variations. The best that we can do is to test the stability of the two-phase deformation against some known necessary conditions for stability, and if any such necessary condition is violated, we can then immediately conclude that the deformation is not an energy minimizer. We have pointed out earlier that satisfaction of the ellipticity condition is a necessary condition for stability with respect to Weierstrass-type perturbations. In this section, we shall consider stability with respect to interfacial perturbations.

We first consider a general finite incompressible elastic body that occupies the region Ω in its reference configuration. We assume that $\partial\Omega = S_u \cup S_t$ where S_u is part of $\partial\Omega$ where displacement is prescribed and S_t is where a dead-load surface traction $\bar{\mathbf{t}}$ is prescribed. The resulting deformation field $\mathbf{x} = \mathbf{x}(\mathbf{X}, t)$ is a kinked deformation with Ω divided into a core region Ω_+ and an outer region $\Omega_- = \Omega\backslash\Omega_+$, the kink surface being denoted by S_p. The t in $\mathbf{x}(\mathbf{X}, t)$ is a time-like variable and is introduced to facilitate calculation of first and second variations of the energy functional. We shall identify $\mathbf{x}(\mathbf{X},0)$ with the primary kinked deformation $\mathbf{x}(\mathbf{X})$ given by (2.1) and write

$$\mathbf{u} = \dot{\mathbf{x}}(\mathbf{X}, 0), \tag{4.1}$$

where a superimposed dot denote partial differentiation with respect to t and $\mathbf{u}$ can be viewed as an incremental displacement field that is superimposed on the primary kinked deformation. We assume that the kink is defined by

$$\mathbf{X} = \mathbf{Y}(\boldsymbol{\alpha}, t), \tag{4.2}$$

where $\boldsymbol{\alpha} = \{\alpha_1, \alpha_2\}^{\mathrm{T}}$ parameterizes the kink.

The total energy corresponding to this kinked deformation is then given by

$$E(t) = \int_{\Omega_+\cup\Omega_-} W(\mathbf{F})\,\mathrm{d}V - \int_{S_t} \bar{\mathbf{t}}\cdot\mathbf{x}\,\mathrm{d}A. \tag{4.3}$$

Due to the propagation of the kink from $\mathbf{Y}(\alpha_1, \alpha_2, t)$ to $\mathbf{Y}(\alpha_1, \alpha_2, t+\delta t)$ alone, the energy would experience an increment

$$\int_{S_p} [W]\{\mathbf{Y}(\boldsymbol{\alpha}, t+\delta t) - \mathbf{Y}(\boldsymbol{\alpha}, t)\}\cdot\mathbf{N}\,\mathrm{d}A + \text{h.o.t.} = \int_{S_p} [W]\dot{\mathbf{Y}}\cdot\mathbf{N}\delta t\,\mathrm{d}A + \text{h.o.t.},$$

where h.o.t. denotes higher order terms, and a superimposed dot denotes partial differentiation with respect to t. Thus,

$$\frac{\mathrm{d}E}{\mathrm{d}t} = \int_{\Omega_+\cup\Omega_-} \frac{\partial W}{\partial F_{iA}}\dot{x}_{i,A}\,\mathrm{d}V + \int_{S_p} [W]\dot{\mathbf{Y}}\cdot\mathbf{N}\,\mathrm{d}A - \int_{S_t} \bar{\mathbf{t}}\cdot\dot{\mathbf{x}}\,\mathrm{d}A. \tag{4.4}$$

Differentiating the constraint $\det\mathbf{F} = 1$ with respect to t, we obtain

$$\mathrm{tr}(\dot{\mathbf{F}}\mathbf{F}^{-1}) = 0, \qquad \mathrm{tr}(\ddot{\mathbf{F}}\mathbf{F}^{-1} + \dot{\mathbf{F}}\mathbf{F}^{-1}\dot{\mathbf{F}}\mathbf{F}^{-1}) = 0. \tag{4.5}$$

Multiplying $(4.5)_1$ by $-p$ and adding it to the first integrand in (4.4), we obtain, after replacing $\bar{\mathbf{t}}$ in the last integrand by $\boldsymbol{\pi}\mathbf{N}$ and applying the divergence theorem,

$$\frac{\mathrm{d}E}{\mathrm{d}t} = \int_{\Omega_+\cup\Omega_-} \left\{-\pi_{iA,A}\dot{x}_i + \left(\frac{\partial W}{\partial F_{iA}} - pF^{-1}_{Ai} - \pi_{iA}\right)\dot{x}_{i,A}\right\}\mathrm{d}V + \int_{S_p} \left\{\pi_{iB}N_B[\dot{x}_i] + [W]\dot{Y}_A N_A\right\}\mathrm{d}A. \tag{4.6}$$

The kink in the current configuration is given by $\mathbf{x} = \mathbf{x}(\mathbf{Y}, t)$. From the fact that its velocity and acceleration must be continuous across the kink surface, we obtain

$$[\dot{x}_i + x_{i,A}\dot{Y}_A] = 0, \qquad [\ddot{x}_i + 2\dot{x}_{i,A}\dot{Y}_A + x_{i,A}\ddot{Y}_A] = 0. \tag{4.7}$$

The $[\dot{x}_i]$ in the second integral in (4.6) can then be expressed in terms of $\dot{Y}_A$ with the aid of $(4.7)_1$. Note that the components $\dot{x}_{i,A}$ of $\dot{\mathbf{F}}$ are not all independent but are subjected to the constraint $(4.5)_1$. Assume that F^{-1}_{11} is nonzero. We may choose p such that

$$\frac{\partial W}{\partial F_{11}} - pF_{11}^{-1} - \pi_{11} = 0. \tag{4.8}$$

Then $\dot{x}_{i,A}$ $(i \neq 1, A \neq 1)$ and $\dot{x}_i$ may be chosen arbitrarily, and $\dot{F}_{11}$ is determined by $(4.5)_1$. Thus, as we expected, by setting the first variation $\mathrm{d}E/\mathrm{d}t$ in (4.6) to zero we obtain the equilibrium equation (2.5), the constitutive relation (2.4) and the jump condition

$$([W]\delta_{AB} - \pi_{iB}[F_{iA}])N_B = 0,$$

which reduces to (2.9) when (2.6) and (2.7) are used.

To derive an expression for the second variation of E, we now return to (4.4). We define a vector-valued function $\phi(\mathbf{X}, t)$ through

$$\boldsymbol{\phi}(\mathbf{X}, t) = \begin{cases} 0 & \text{on } \partial\Omega, \\ \dot{\mathbf{Y}} & \text{on } \mathbf{X} = \mathbf{Y}(\boldsymbol{\alpha}, t). \end{cases} \tag{4.9}$$

The above definition implies

$$\phi_A(\mathbf{Y}(\boldsymbol{\alpha}, t), t) = \dot{Y}_A, \qquad \dot{\phi}_A = \ddot{Y}_A - \phi_{A,B}\phi_B. \tag{4.10}$$

It then follows that

$$\int_{S_p} W^- \dot{\mathbf{Y}} \cdot \mathbf{N}\,\mathrm{d}A = \int_{S_p} W^- \boldsymbol{\phi} \cdot \mathbf{N}\,\mathrm{d}A = \int_{\partial\Omega^-} W^- \boldsymbol{\phi} \cdot \mathbf{N}\,\mathrm{d}A = \int_{\Omega^-} \frac{\partial}{\partial X_A}(W\phi_A)\,\mathrm{d}V.$$

Similarly, we have

$$\int_{S_p} W^+ \dot{\mathbf{Y}} \cdot \mathbf{N}\,\mathrm{d}A = -\int_{\Omega^+} \frac{\partial}{\partial X_A}(W\phi_A)\,\mathrm{d}V.$$

Thus, (4.4) can be written as

$$\frac{\mathrm{d}E}{\mathrm{d}t} = \int_{\Omega_+ \cup \Omega_-} \left\{ \frac{\partial W}{\partial F_{iA}} \dot{x}_{i,A} + \frac{\partial}{\partial X_A}(W\phi_A) \right\} \mathrm{d}V - \int_{S_t} \bar{\mathbf{t}} \cdot \dot{\mathbf{x}}\,\mathrm{d}A. \tag{4.11}$$

Differentiating (4.11) again with respect to t and arguing in the same manner as that leading from (4.3) to (4.4), we obtain

$$\begin{aligned} \frac{\mathrm{d}^2 E}{\mathrm{d}t^2} = & \int_{\Omega_+ \cup \Omega_-} \frac{\partial^2 W}{\partial F_{iA} \partial F_{jB}} \dot{x}_{i,A}\dot{x}_{j,B} + \frac{\partial W}{\partial F_{iA}} \ddot{x}_{i,A} + \frac{\partial}{\partial X_A}\left(\frac{\partial W}{\partial F_{jB}} \dot{x}_{j,B}\phi_A + W\dot{\phi}_A \right) \\ & + \int_{S_p} \left[\frac{\partial W}{\partial F_{iA}} \dot{x}_{i,A} + W_{,A}\phi_A + W\phi_{A,A} \right] \dot{\mathbf{Y}} \cdot \mathbf{N}\,\mathrm{d}A - \int_{S_t} \bar{\mathbf{t}} \cdot \ddot{\mathbf{x}}\,\mathrm{d}A. \end{aligned} \tag{4.12}$$

Applying the divergence theorem to the third term in the first integral and noting that on the outer boundary $\phi_A = 0$, $\dot{\phi}_A = 0$, we obtain

$$\begin{aligned} \frac{\mathrm{d}^2 E}{\mathrm{d}t^2} = & \int_{\Omega_+ \cup \Omega_-} \left\{ \frac{\partial^2 W}{\partial F_{iA} \partial F_{jB}} \dot{x}_{i,A}\dot{x}_{j,B} + (\pi_{iA} + pF_{Ai}^{-1})\ddot{x}_{i,A} \right\} \mathrm{d}V + \int_{S_p} [W\dot{\phi}_A]N_A\,\mathrm{d}A \\ & + \int_{S_p} [2(\pi_{iA} + pF_{Ai}^{-1})\dot{x}_{i,A} + W_{,A}\phi_A + W\phi_{A,A}]\phi_B N_B\,\mathrm{d}A - \int_{S_t} \bar{\mathbf{t}} \cdot \ddot{\mathbf{x}}\,\mathrm{d}A, \end{aligned} \tag{4.13}$$

where we have also used $(2.4)_2$ to eliminate the first order derivative of W. The second order derivative of W in (4.13) can be eliminated using

$$\dot{\pi}_{iA} = \frac{\partial^2 W}{\partial F_{iA} \partial F_{jB}} \dot{x}_{j,B} - \dot{p}F_{Ai}^{-1} + pF_{Aj}^{-1}F_{Bi}^{-1}\dot{F}_{j,B}$$

obtained from $(2.4)_2$, and the last term in (4.13) can be eliminated with the aid of the following expression:

$$\int_{S_t} \bar{\mathbf{t}} \cdot \ddot{\mathbf{x}} \, \mathrm{d}A = \int_{S_t} \boldsymbol{\pi}\mathbf{N} \cdot \ddot{\mathbf{x}} \, \mathrm{d}A = \int_{\Omega_+ \cup \Omega_-} \frac{\partial}{\partial X_A}(\pi_{iA}\ddot{x}_i) \, \mathrm{d}V - \int_{S_p} [\pi_{iA} N_A \ddot{x}_i] \, \mathrm{d}A$$
$$= \int_{\Omega_+ \cup \Omega_-} \pi_{iA}\ddot{x}_{i,A} \, \mathrm{d}V - \int_{S_p} \pi_{iA} N_A [\ddot{x}_i] \, \mathrm{d}A.$$

With the further use of (4.5), $(4.7)_2$, and $(4.10)_2$ Eq. (4.13) may be reduced to

$$\frac{\mathrm{d}^2 E}{\mathrm{d}t^2} = \int_{\Omega_+ \cup \Omega_-} \dot{\pi}_{iA}\dot{x}_{i,A} \, \mathrm{d}V + \int_{S_p} \{[2(\pi_{iA} + pF^{-1}_{Ai})\dot{x}_{i,A}\phi_B N_B + W(\phi_{B,B}\phi_A N_A - \phi_{A,B}\phi_B N_A)]$$
$$- 2\pi_{iA} N_A [\dot{x}_{i,B}]\phi_B\} \, \mathrm{d}A. \tag{4.14}$$

The volume integral above can be converted into a surface integral by first writing $\dot{\pi}_{iA}\dot{x}_{i,A}$ as $(\dot{\pi}_{iA}\dot{x}_i)_{,A}$ and then applying the divergence theorem. On evaluating the resulting expression at $t = 0$ and making use of (4.1), we obtain the following expression for the second variation of the energy functional:

$$\delta^2 E \equiv \left.\frac{\mathrm{d}^2 E}{\mathrm{d}t^2}\right|_{t=0} = \int_{S_p} \{[\dot{\pi}_{iA}u_i]N_A + [2\pi_{iA}u_{i,A}]\phi_B N_B + [W](\phi_{B,B}\phi_A N_A - \phi_{A,B}\phi_B N_A) - 2\pi_{iA} N_A [u_{i,B}]\phi_B\} \, \mathrm{d}A, \tag{4.15}$$

where here and hereafter $\boldsymbol{\phi}$ and $\dot{\boldsymbol{\pi}}$ are evaluated at $t = 0$. This expression has previously been obtained by Fu and Freidin (2004) using a different procedure in their studies of stress induced phase transformations.

To facilitate computations to be carried out later, we now rewrite the above expression for the second variation by transforming the variables of integration from (X_A) to (x_i). To this end, we introduce

$$\chi_{ij} = \dot{\pi}_{iA}F_{jA}, \qquad \sigma_{ij} = \pi_{iA}F_{jA}, \qquad \psi_i = F_{iB}\phi_B, \qquad \Gamma = \frac{\mathrm{d}A}{\mathrm{d}a}\phi_A N_A, \tag{4.16}$$

and note that

$$N_A = \frac{\mathrm{d}a}{\mathrm{d}A}F_{iA}n_i, \qquad [\psi_i] = c_i\Gamma, \qquad [u_i] = -c_i\Gamma, \tag{4.17}$$

where use has been made of (2.7), (2.13) and $(4.7)_1$ evaluated at $t = 0$, and dA and da are two corresponding area elements in the undeformed and kinked configurations, respectively. With the use of these relations, (4.15) can be rewritten as

$$\delta^2 E = \int_{s_p} \{[\chi_{ij}n_j u_i] + 2\Gamma[\sigma_{ij}u_{i,j}] + [W](\psi_{j,j}\Gamma - \psi_{i,j}\psi_j n_i) - 2\sigma_{ij}n_j[u_{i,k}\psi_k]\} \, \mathrm{d}a, \tag{4.18}$$

where s_p is the image of the kink surface relative to the coordinate system (x_i). We note that although ψ_i is discontinuous across the kink surface, the expressions $\psi_{j,j}\Gamma$ and $\psi_{i,j}\psi_j n_i$ are both continuous across the kink surface since their counterparts in (4.15) are clearly continuous.

We now specialize to the plane-strain deformation considered in the previous section. In this case, we introduce new variables y_1, y_2 through

$$y_1 = \mathbf{m} \cdot \mathbf{x}, \qquad y_2 = \mathbf{n} \cdot \mathbf{x},$$

and without loss of generality we assume that the kink corresponds to $y_2 = 0$. A straightforward manipulation followed by the use of (2.9) and (3.5) shows that (4.18) in this case reduces to

$$\delta^2 E = \int_{s_p} \left\{ [\mathbf{u} \cdot \boldsymbol{\chi}\mathbf{n}] + 2\Gamma\left[\frac{\partial \mathbf{u}}{\partial y_1} \cdot \boldsymbol{\sigma}\mathbf{m}\right] - 2k\Gamma\frac{\partial \mathbf{u}^-}{\partial y_1} \cdot \boldsymbol{\sigma}\mathbf{n} + [W]\frac{\partial}{\partial y_1}(\mathbf{m} \cdot \boldsymbol{\psi}^+\Gamma) \right\} \mathrm{d}a. \tag{4.19}$$

Finally, we assume that the perturbations/variations take the following normal-mode form:

$$\Gamma = \gamma e^{iy_1} + \text{c.c.}, \qquad \mathbf{u}(\mathbf{X}) = \mathbf{z}(y_2)e^{iy_1} + \text{c.c.}, \tag{4.20}$$

where γ and $\mathbf{z}$ are to be determined, and c.c. denotes the complex conjugate of the preceding term. The amplitude function $\mathbf{z}(y_2)$ is required to satisfy the continuity condition

$$[\mathbf{z}] = -k\mathbf{m}\gamma, \tag{4.21}$$

obtained from (4.17)$_3$, the equilibrium equation $\chi_{ij,j} = 0$ and the decay condition $\mathbf{z}(\pm\infty) = 0$.

We now introduce the surface-impedance tensors $\mathbf{M}^{\pm}$ through

$$\boldsymbol{\chi}^{+}\mathbf{n} = \widehat{\mathbf{M}}^{+}\mathbf{z}^{+}e^{iy_1} + \text{c.c.}, \qquad \boldsymbol{\chi}^{-}\mathbf{n} = -\mathbf{M}^{-}\mathbf{z}^{-}e^{iy_1} + \text{c.c.}, \tag{4.22}$$

where a superimposed hat signifies complex conjugation. The surface-impedance tensor was first introduced by Ingerbrigtsen and Tonning (1969) and it has played an important role in the development of surface-wave theory and theory of anisotropic elasticity. It has an explicit integral representation in terms of the elastic moduli defined by (2.14) even in the most general case; see Barnett and Lothe (1973) and Fu (in press) for the formulae for compressible and incompressible materials, respectively. For plane-strain deformations, explicit formulae are given by Fu (2005) and Fu and Brookes (in press) for incompressible and compressible materials, respectively.

The integral in (4.19) is now replaced by an average over one period of the normal-mode variation:

$$\delta^2 E = \frac{1}{2\pi}\int_0^{2\pi}\left\{[\mathbf{u}\cdot\boldsymbol{\chi}\mathbf{n}] + 2\Gamma\left[\frac{\partial\mathbf{u}}{\partial y_1}\cdot\boldsymbol{\sigma}\mathbf{m}\right] - 2k\Gamma\frac{\partial\mathbf{u}^{-}}{\partial y_1}\cdot\boldsymbol{\sigma}\mathbf{n}\right\}dy_1. \tag{4.23}$$

On substituting (4.20) and (4.22) into (4.23), we obtain

$$\frac{1}{2}\delta^2 E = \hat{\mathbf{z}}^{-}\cdot\mathbf{P}\mathbf{z}^{-} + \gamma\hat{\mathbf{z}}^{-}\cdot\mathbf{g} + \hat{\mathbf{g}}\cdot\mathbf{z}^{-}\hat{\gamma} + |\gamma|^2\mathbf{c}\cdot\widehat{\mathbf{M}}^{+}\mathbf{c} = \hat{\mathbf{w}}\cdot\mathbf{H}\mathbf{w}, \tag{4.24}$$

where

$$\mathbf{P} = \widehat{\mathbf{M}}^{+} + \mathbf{M}^{-}, \qquad \mathbf{H} = \begin{pmatrix}\mathbf{P} & \mathbf{g}\\ \hat{\mathbf{g}}^{\mathrm{T}} & \mathbf{c}\cdot\widehat{\mathbf{M}}^{+}\mathbf{c}\end{pmatrix}, \qquad \mathbf{w} = \begin{pmatrix}\mathbf{z}^{-}\\ \gamma\end{pmatrix},$$
$$\mathbf{g} = -\widehat{\mathbf{M}}^{+}\mathbf{c} - i(\boldsymbol{\beta} - k\boldsymbol{\sigma}\mathbf{n}), \qquad \boldsymbol{\beta} = [\boldsymbol{\sigma}\mathbf{m}] = k[\boldsymbol{\sigma}\mathbf{c}]. \tag{4.25}$$

Fu and Freidin (2004) did not apply the variable transformation $(X_A) \to (x_i)$ to the integral in (4.15). As a result, their final expression for the second variation was in terms of $\mathbf{f}$, $\mathbf{N}$ and $\boldsymbol{\pi}$. We have verified that their expression (6.18) can be converted to our expression (4.24) with the aid of (4.16) and (4.17).

It is well-known that when the strong ellipticity condition is satisfied, the surface-impedance matrices, and hence $\mathbf{P}$, are Hermitian. It then follows that the kinked solution is stable with respect to the interfacial perturbations considered if all the eigenvalues of the Hermitian matrix $\mathbf{H}$ are positive and is unstable if at least one of them is negative.

As an illustrative example, we now specialize to the material model (3.2). We have

$$\sigma_{ij} = B_{ij} + 2\{\gamma_1(I_4 - 1) + \gamma_2(I_4 - 1)^2\}a_i a_j - p\delta_{ij}, \tag{4.26}$$

$$\mathscr{A}_{jilk} = \delta_{ik}B_{jl} + 4\{\gamma_1 + 2\gamma_2(I_4 - 1)\}a_j a_i a_l a_k + 2\{\gamma_1(I_4 - 1) + \gamma_2(I_4 - 1)^2\}\delta_{ik}a_j a_l. \tag{4.27}$$

We see from (4.25)$_2$ that to compute $\mathbf{H}$ it only remains to find an expression for the two surface-impedance matrices (tensors). It is known that such matrices are invariant with respect to rotations of $\mathbf{n}$ and $\mathbf{m}$ in the x_1x_2-plane (see, e.g., Mielke and Fu, 2004). This means that for the purpose of computing the surface-impedance matrices, we may simply take $\mathbf{m} = (1,0)^{\mathrm{T}}$, $\mathbf{n} = (0,1)^{\mathrm{T}}$. Thus, the explicit formulae given by Fu (2005) can directly be applied here. We have

$$\mathbf{M} = \begin{pmatrix} M_1 & M_3 + \mathrm{i}M_4 \\ M_3 - \mathrm{i}M_4 & M_2 \end{pmatrix}, \tag{4.28}$$

and

$$\begin{aligned} &M_1 = d_{22}\sqrt{-w_2}, \qquad w_2 = 2\omega^{1/3}\cos(\phi + 2\pi/3) - \frac{2}{3}r, \qquad M_4 = \frac{M_1^2}{2d_{22}} + \frac{b_3}{2}, \\ &M_3 = \frac{d_{22}}{M_1}\left(\frac{b_1}{2d_{22}}M_1^2 + \frac{b_1 b_3}{2} - b_4\right), \qquad M_2 = \frac{1}{d_{22}}M_1 M_4 - b_2 M_1 + b_1 M_3, \end{aligned} \tag{4.29}$$

where

$$\begin{aligned} &r = (2d_{12}d_{22} - 6d_{26}^2 + 4d_{66}d_{22})/d_{22}^2, \\ &s = \{4d_{16}d_{22}^2 - 4d_{26}(d_{12}d_{22} - 2d_{26}^2 + 2d_{22}d_{66})\}/d_{22}^3, \\ &h = \{d_{11}d_{22}^3 + d_{26}(-4d_{16}d_{22}^2 + 2d_{12}d_{22}d_{26} - 3d_{26}^3 + 4d_{22}d_{26}d_{66})\}/d_{22}^4, \\ &\omega = \frac{1}{27}(12h + r^2)^{\frac{3}{2}}, \qquad \cos 3\phi = \frac{27}{2}(12h + r^2)^{-\frac{3}{2}}\left(\frac{2}{27}r^3 + s^2 - \frac{8}{3}rh\right), \\ &b_1 = -2d_{26}/d_{22}, \qquad b_2 = d_{12}/d_{22}, \\ &b_3 = 4d_{26}^2/d_{22} - 4d_{66}, \qquad b_4 = 2d_{16} - 2d_{12}d_{26}/d_{22}, \end{aligned} \tag{4.30}$$

and

$$\begin{aligned} &d_{11} = \mathscr{A}_{1111}, \qquad d_{22} = \mathscr{A}_{2121}, \qquad 2d_{26} = \mathscr{A}_{1121} - \mathscr{A}_{2122}, \\ &d_{12} = -\mathscr{A}_{1122} - p, \qquad 2d_{16} = \mathscr{A}_{1222} - \mathscr{A}_{1112}, \qquad 4d_{66} = \mathscr{A}_{1111} + \mathscr{A}_{2222} - 2\mathscr{A}_{1122} + 2p. \end{aligned}$$

To find $\mathbf{M}^+$ or $\mathbf{M}^-$, we simply replace the $\mathscr{A}_{jilk}, p$ above by $\mathscr{A}^+_{jilk}, p^+$ or $\mathscr{A}^-_{jilk}, p^-$, respectively.

We have yet to verify that the deformation in the kink band also satisfies the strong ellipticity condition. One way to verify this is to use the fact the $\mathbf{M}^+$ is Hermitian only if the strong ellipticity condition is satisfied. Alternatively, the strong ellipticity condition is satisfied only if the expression for $\cos 3\phi$ given by (4.30) takes values in $[-1,1]$. Using this latter criterion, we find that when γ_2 is fixed at 4.5 and λ in (3.4) taken to correspond to the right noses of the closed curves in Fig. 2, the strong ellipticity is satisfied for γ_1 up to approximately 0.02512.

For the four sets of material parameters used in Fig. 2, the three eigenvalues of H are found as follows:

$$\begin{aligned} &\gamma_1 = 0 : (0.003032, 0.4702, 0.6880), \\ &\gamma_1 = 0.01 : (0.001815, 0.4573, 0.5797), \\ &\gamma_1 = 0.02 : (0.0008577, 0.3155, 0.4497), \\ &\gamma_1 = 0.0251 : (0.0004845, 0.1894, 0.3706). \end{aligned}$$

Thus, for $\gamma_2 = 0.45$, $0 \leqslant \gamma_1 < 0.0251$, the kinked solution is stable with respect to interfacial perturbations.

5. Conclusion

In this paper, we have presented a rational continuum mechanical framework for modelling kink-band formations. We take the point of view that in an ideal situation when the material is free from imperfections, formation of kink bands is a discontinuous, dynamic process and can be induced by a large amplitude perturbation well before the strong ellipticity condition is violated. We also believe that a fully developed kink surface is a strong discontinuity across which the deformation gradient generally suffers a finite jump which cannot adequately be described by an incremental theory. This point of view seems to be consistent with the available experimental results; see, for instance, Kyriakides et al. (1995), Moran et al. (1995), Moran and Shih (1998), and Wadee et al. (2004). In contrast with most of the previous theoretical models, we use the Maxwell relation as an equilibrium condition. As a result, once the strain–energy function is chosen, the kink propagation stress, the kink orientation angle and the fibre direction within the kink band are all determined by our theoretical model. A good theoretical model for a fully developed stable kink band should also satisfy certain stability criteria. We have presented simple formulae that can be used to test the strong ellipticity condition and stability with respect to interfacial perturbations.

In this paper, our focus has been on the explanation of a general methodology for modelling kink-band formation using a simple form of the strain–energy function. We observe that the numerical results (3.23) from our illustrative example compare poorly with the empirical relation

$$\beta = \frac{\alpha}{2}, \tag{5.1}$$

and the usually reported result $\beta \approx 5$–$15°$. We note, however, that (5.1) was only advanced for composites that are not only incompressible but also inextensible along the fibre direction (Chaplin, 1977). We expect that the predicted values of α and β would be strongly dependent on the form of the strain–energy function used. It would be of interest to check, under the present theoretical framework, whether (5.1) is an exact relation for the type of composites for which it is intended. Ultimately, for any given unidirectional fibre-reinforced composite, we would like to build a model (that is, to find a strain–energy function) that can predict what have been observed in experiments and what might be expected in other loading conditions. These tasks will be carried out in future studies.

Acknowledgements

The research reported in this paper is supported by a joint grant from the Royal Society and the National Natural Science Foundation of China under their Joint Project Scheme. We thank Professor A.B. Freidin for stimulating discussions on various aspects of stress-induced phase transformations.

References

Abeyaratne, R., 1983. An admissibility condition for equilibrium shocks in finite elasticity. J. Elast. 13, 175–184.

Barnett, D.M., Lothe, J., 1973. Synthesis of the sextic and the integral formalism for dislocations, Greens function and surface waves in anisotropic elastic solids. Phys. Norv. 7, 13–19.

Berbinau, P., Soutis, C., Guz, I.A., 1999. Compressive failure of 0° unidirectional carbon-fibre-reinforced plastic (CFRP) laminates by fibre microbuckling. Comp. Sci. Tech. 59, 1451–1455.

Budiansky, B., Fleck, N.A., 1993. Compressive failure of fibre composites. J. Mech. Phys. Solids 41, 183–211.

Budiansky, B., Fleck, N.A., 1994. Compressive kinking of fibre composites: a topical review. Appl. Mech. Rev. 47 (6, Part 2), S246–S250.

Budiansky, B., Fleck, N.A., Amazigo, J.C., 1998. On kink-band propagation in fibre composites. J. Mech. Phys. Solids 46, 1637–1653.

Chaplin, C.R., 1977. Compressive fracture in unidirectional glass-reinforced plastics. J. Mater. Sci. 12, 347–352.

Cherkaev, A., 1991. Variational Methods for Structural Optimization. Springer, Berlin.

Christoffersen, J., Jensen, H.M., 1996. Kink band analysis accounting for the microstructure of fiber reinforced materials. Mech. Mater. 24, 305–315.

Chung, I., Weitsman, Y., 1995. On the buckling/kinking compressive failure of fibrous composites. Int. J. Solids Struct. 32, 2329–2344.

Dao, M., Asaro, R.J., 1996. On the critical conditions of kink band formation in fiber composites with ductile matrix. Scr. Mater. 34, 1771–1777.
Drapier, S., Grandidier, J.-C., Potier-Ferry, M., 2001. A structural approach of plastic microbuckling in long fibre composites: comparison with theoretical and experimental results. Int. J. Solids Struct. 38, 3877–3904.
Ericksen, J.L., 1975. Equilibrium of bars. J. Elast. 5, 191–201.
Fleck, N.A., 1997. Compressive failure of fibre composites. Adv. Appl. Mech. 33, 43–117.
Freidin, A.B., Chiskis, A.M., 1994a. Phase transition zones in nonlinear elastic isotropic materials. Part 1: Basic relations. Izv. Ran. Mekhanika Tverdogo Tela (Mechanics of Solids) 29, 91–109.
Freidin, A.B., Chiskis, A.M., 1994b. Phase transition zones in nonlinear elastic isotropic materials. Part 2: Incompressible materials with a potential depending on one of deformation invariants. Izv. Ran. Mekhanika Tverdogo Tela (Mechanics of Solids) 29, 46–58.
Freidin, A.B., Vilchevskaya, E.N., Sharipova, L.L., 2002. Two-phase deformations within the framework of phase transition zones. Theor. Appl. Mech. (Belgrade) 28–29, 149–172.
Fu, Y.B., 2005. An explicit expression for the surface-impedance matrix of a generally anisotropic incompressible elastic material in a state of plane strain. Int. J. Non-linear Mech. 40, 229–239.
Fu, Y.B., in press. An integral representation of the surface-impedance tensor for incompressible elastic materials. J. Elast.
Fu, Y.B., Freidin, A.B., 2004. Characterization and stability of two-phase piecewise-homogeneous deformations. Proc. Roy. Soc. London A 460, 3065–3094.
Fu, Y.B., Brookes, D.W., in press. An explicit expression for the surface-impedance matrix of a generally anisotropic compressible elastic material in a state of plane strain. IMA J. Appl. Math.
Grandidier, J.-C., Ferron, G., Potier-Ferry, M., 1992. Microbuckling and strength in long-fiber composites: theory and experiments. Int. J. Solids Struct. 29, 1753–1761.
Guynn, E.G., Ochoa, O.O., Bradley, W.L., 1992. A parametric study of variables that affect fiber microbuckling initiation in composite laminates. Part I: Analyses. J. Compos. Mater. 26, 1594–1616.
Hsu, S.-Y., Vogler, T.J., Kyriakides, S., 1999. On the axial propagation of kink bands in fiber composites. Part II: Analysis. Int. J. Solids Struct. 36, 575–595.
Hunt, G.W., Peletier, M.A., Wadee, M.A., 2000. The Maxwell stability criterion in pseudo-energy models of kink banding. J. Strut. Geol. 22, 669–681.
Ingerbrigtsen, K.A., Tonning, A., 1969. Elastic surface waves in crystals. Phys. Rev. 184, 942–951.
Jensen, H.M., 1999. Analysis of compressive failure of layered materials by kink band broadening. Int. J. Solids Struct. 36, 3427–3441.
Jensen, H.M., Christoffersen, J., 1997. Kink band formation in fibre reinforced materials. J. Mech. Phys. Solids 45, 1121–1136.
Knowles, J.K., Sternberg, E., 1978. On the failure of ellipticity and the emergence of discontinuous deformation gradients in plane finite elastostatics. J. Elast. 8, 329–379.
Kyriakides, S., Arseculerane, R., Perry, E., Liechti, K.M., 1995. On the compressive failure of fibre reinforced composites. Int. J. Solids Struct. 32, 689–738.
Kyriakides, S., Ruff, A.E., 1997. Aspects of the failure and postfailure of fiber composites in compression. J. Compos. Mater. 31 (20), 2000–2037.
Liu, X.H., Moran, P.M., Shih, C.F., 1996. The mechanics of compressive kinking in unidirectional fiber reinforced ductile matrix composites. Compos. Eng. B 27 (Part B), 553–560.
Merodio, J., Ogden, R.W., 2002. Material instabilities in fiber-reinforced nonlinearly elastic solids under plane deformation. Arch. Mech. 54, 525–552.
Merodio, J., Ogden, R.W., 2003a. Instabilities and loss of ellipticity in fiber-reinforced compressible non-linearly elastic solids under plane deformation. Int. J. Solids Struct. 40, 4707–4727.
Merodio, J., Ogden, R.W., 2003b. A note on strong ellipticity for transversely isotropic linearly elastic solids. Q.J. Mech. Appl. Math. 56, 589–591.
Merodio, J., Ogden, R.W., 2005. Mechanical response of fiber-reinforced incompressible nonlinearly elastic solids. Int. J. Non-Linear Mech. 40, 213–227.
Merodio, J., Pence, T.J., 2001a. Kink surfaces in a directionally reinforced neo-Hookean material under plane deformation: I. Mechanical equilibrium. J. Elast. 62, 119–144.
Merodio, J., Pence, T.J., 2001b. Kink surfaces in a directionally reinforced neo-Hookean material under plane deformation: II. Kink band stability and maximally dissipative band broadening. J. Elast. 62, 145–170.
Mielke, A., Sprenger, P., 1998. Quasiconvexity at the boundary and a simple variational formulation of Agmon's condition. J. Elast. 51, 23–41.
Moran, P.M., Liu, X.H., Shih, C.F., 1995. Kink band formation and band broadening in fibre composites under compressive loading. Acta Metall. Mater. 43, 2943–2958.
Moran, P.M., Shih, C.F., 1998. Kink band formation and band broadening in ductile matrix fiber composites: experiments and analysis. Int. J. Solids Struct. 35, 1709–1722.

Mielke, A., Fu, Y.B., 2004. Uniqueness of surface-wave speed: a proof that is independent of the Stroh formalism. Math. Mech. Solids 9, 5–15.
Qiu, G.Y., Pence, T.J., 1997. Loss of ellipticity in plane deformations of a simple directionally reinforced incompressible nonlinear elastic solid. J. Elast. 49, 31–63.
Schapery, R.A., 1995. Predication of compressive strength and kink bands in composites using a work potential. Int. J. Solids Struct. 32, 739–765.
Simpson, H.C., Spector, S.J., 1989. Necessary conditions at the boundary for minimizers in finite elasticity. Arch. Ration. Mech. Anal. 107, 105–125.
Simpson, H.C., Spector, S.J., 1991. Some necessary conditions at an internal boundary for minimizers in finite elasticity. J. Elast. 26, 203–222.
Sivashanker, S., Fleck, N.A., Sutcliffe, M.P.F., 1996. Microbuckle propagation in a unidirectional carbon fibre—epoxy matrix composite. Acta Metall. Mater. 44 (7), 2581–2590.
Spencer, A.J.M., 1972. Deformations of Fibre-reinforced Materials. Oxford University Press.
Sutcliffe, M.P.F., Fleck, N.A., 1994. Microbuckle propagation in carbon fibre—epoxy composites. Acta Metall. Mater. 42 (7), 2219–2231.
Triantafyllidis, N., Abeyaratne, R.C., 1983. Instability of a finitely deformed fiber-reinforced elastic material. J. Appl. Mech. 50, 149–156.
Vogler, T.J., Kyriakides, S., 1997. Initiation and axial propagation of kink bands in fiber composites. Acta Mater. 45, 2443–2454.
Vogler, T.J., Kyriakides, S., 1999. On the axial propagation of kink bands in fiber composites. Part I: Experiments. Int. J. Solids Struct. 36, 557–574.
Vogler, T.J., Kyriakides, S., 2001. On the initiation and growth of kink bands in fiber composites. Part I: Experiments. Int. J. Solids Struct. 38, 2639–2651.
Vogler, T.J., Hsu, S.Y., Kyriakides, S., 2001. On the initiation and growth of kink bands in fiber composites. Part II: Analysis. Int. J. Solids Struct. 38, 2653–2682.
Wadee, M.A., Hunt, G.W., Peletier, M.A., 2004. Kink band instability in layered structures. J. Mech. Phys. Solids 52, 1071–1091.
Walton, J.R., Wilber, J.P., 2003. Sufficient conditions for strong ellipticity for a class of anisotropic materials. Int. J. Non-Linear Mech. 38, 441–455.
Yin, W.L., 1992. A new theory of kink band formation. AIAA-92-2552-CP, pp. 3028–3035.